Acta Geochim (2023) 42:1124–1129
https://doi.org/10.1007/s11631-023-00638-2

SHORT COMMUNICATION

2.7-Ga-old mafic dike in the Trans-North China Orogen of the North China Craton and its tectonic significance

Haiyan Liu[1] · **Chong Peng**[1,2,3]

Received: 8 August 2023 / Revised: 18 August 2023 / Accepted: 30 August 2023 / Published online: 19 September 2023

Abstract We studied an Archean mafic dike in the Trans-North China Orogen of the North China Craton, which has a magmatic age of 2701 ± 83 Ma and is currently the oldest mafic dike in the North China Craton. Such an old dike is extremely rare in the world. The presence of mafic dikes indicates that the North China Craton was in a tensional tectonic environment at 2.7 Ga. Geochemical characteristics reveal that this mafic dike belongs to continental tholeiitic basalt. Results from Hf isotope analysis reveal that the mafic dike originates from a depleted mantle. The plate assembly in the North China landmass was realized during the Archean era (2.7 Ga), and a thick and stable continental crust was formed. Therefore, the first cratonization of the North China Craton was completed before 2.7 Ga. The intrusion of the 2.7-Ga-old mafic dike from the deep lithospheric mantle of the continent indicates that the North China Craton has undergone a period of extensional tectonic activity. This event marks a significant extensional event that occurred after the cratonization of the North China Craton.

Keywords Archean · Mafic dike · Trans-North China Orogen · North China Craton · Hf · Cratonization

1 Introduction

Mafic dikes are formed by the penetration of basaltic magma from the Earth's mantle along tensile fractures that occur during continental extension. This process is a significant indicator of both supercontinent reconstruction and mantle plumes (Buchan et al. 2001; Ernst et al. 2010; Stark et al. 2018) and can be used to restore the tectonic environment and determine the direction of paleo-stress during magma emplacement (Halls and Zhang 1998; Hoek and Seitz 1995; Hou 2012). Mafic dikes are associated with the process of crustal extension in the craton, such as subduction (back-arc expansion), post-metallogenic collapse, plume, and rift during supercontinent rupture (Stark et al. 2018). Mafic dikes are closely linked to the early history of cratons, shortly after the assembly and stabilization of crustal blocks. For example, a dike emplacement in the North China Craton (NCC) approximately 2516–2504 Ma ago suggests the presence of deep subcontinental lithosphere and provides a timeline for the Neoarchean cratonization (Li et al. 2010). The discovery of the currently oldest mafic dike on the NCC, with a precise age of 2701 ± 83 Ma, suggests that the Neoarchean cratonization may have occurred earlier than previously thought, around 2.7 Ga ago.

The NCC is the largest and oldest craton in eastern Eurasia, with a zircon age record dating back 4.1–4.0 Ga (Fig. 1a) and an evolutionary history of over 3.8 Ga (Kusky et al. 2001; Peng et al. 2016, 2020, 2021). The NCC is divided into eastern and western continental blocks

✉ Chong Peng
pengchong13@mails.jlu.edu.cn

Haiyan Liu
haiyanliu@sxnu.edu.cn

1 College of Geographical Sciences, Shanxi Normal University, Taiyuan 030031, China

2 Key Laboratory of Deep-Earth Dynamics of Ministry of Natural Resources, Institute of Geology, Chinese Academy of Geological Sciences, Beijing 100037, China

3 School of GeoSciences, University of Edinburgh, Edinburgh EH9 3JW, UK

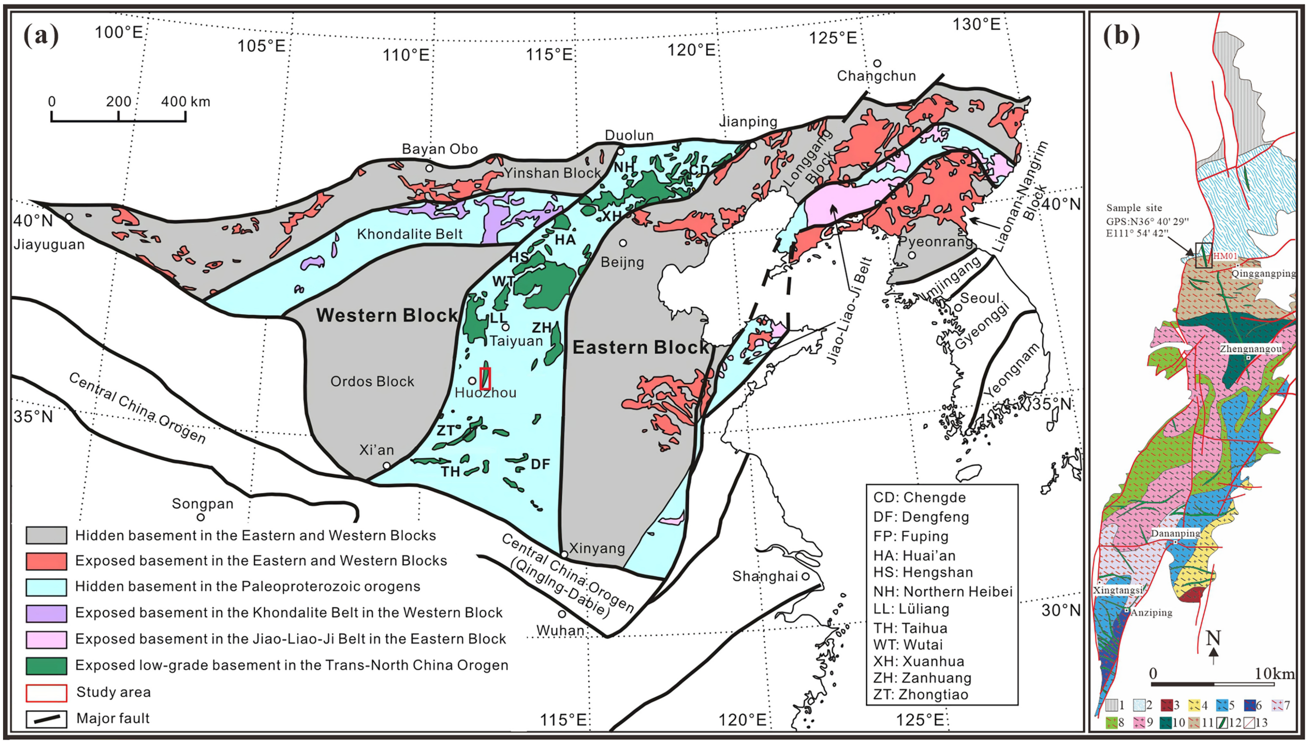

Fig. 1 **a** Tectonic subdivision of NCC (modified after Peng et al. 2023; Wang et al. 2022; Xu and Liu 2019; Zhao et al. 2012). **b** Geological map of the Huozhou metamorphic complex generated from a 1:200,000 scale geological map of China, Linfen sheet (modified after Peng et al. 2023; Wang et al. 2022). (1) Bolianghe Formation, (2) Shigaoshan Formation, (3) Jiehekou Group, (4) Pengpenggou Formation of the Huoxian Group, (5) Xiaonanping Formation of the Huoxian Group, (6) Anziping gneiss, (7) Xingtangsi gneiss, (8) Dananping Formation of the Huoxian Group, (9) Anziping Formation of the Huoxian Group, (10) Zhengnangou gneiss, (11) Qinggangping gneiss, (12) Mafic dike, (13) Fault

by the Trans-North China Orogen (TNCO), which extends 1200 km in the north–south direction (Peng et al. 2023) (Fig. 1a).

The mafic dike discovered in our study is situated in the eastern part of Huozhou, within the central region of the TNCO (Fig. 1a, b). A significant number of diabase wall groups were found in this area, with the diabase wall distributed in a north–south direction, approximately 2 km long and 25 m wide. The rock wall is visible along a manually excavated mountain road (Fig. 1b), the diabase wall was later intruded by granite dating back approximately 2200 Ma ago (Peng et al. 2023).

The Archean mafic dike samples analyzed in this study were collected from Qinggangping Village, Huozhou, Shanxi Province (Fig. 1b, 36°40′29″ N, 111°54′ 42″ E). As illustrated in Fig. S1, the rock samples from the Qinggangping mafic dike (HM01) appear grayish-green (Fig. S1a) and present a semi-automorphic granular structure, diabase structure, metasomatic residual structure, and massive structure (Fig. S1b–d) The minerals are primarily plagioclase (50–55 %) and diopside (20–25 %) (Fig. S1e). The plagioclase particles are approximately 0.45–2.50 mm in size and consist of semi-automorphic plates with wide patchy double crystals. The crystal surface appears turbid. Sodium zoisite and sericite are present in abundance, and local formations take the shape of a triangular grid (Fig. S1f). The diopside particles are approximately 0.15–1.50 mm in size. These are semi-automorphic crystals with well-developed pyroxene cleavage (Fig. S1e). Simple twin crystals that are damaged are found in low numbers. Secondary actinolization, chloritization, epidotization, carbonation, precipitation of iron, and filling in the plagioclase framework all contributed to the formation of the diabase structure.

The LA-ICP-MS zircon U–Pb dating analysis of the samples was conducted at the Beijing CreaTech Testing Technology Co., Ltd. The Agilent 7500 ICP-MS instrument equipped with its supporting resolution 193 nm excimer laser ablation system (see Supplementary Text for the measurement process) was used for zircon dating analysis. The zircon particle size ranged from 80 to 180 μm, and the width ranged from 40 to 70 μm. The cathodoluminescence (CL) images of the zircons revealed tabular bands (Fig. 2). All zircons have high U and Th contents, and high Th/U ratios (up to 1.58), and only two zircons were characterized by Th/U ratios less than 0.4. The rare earth element composition presented a typical magmatic origin. Ce positive anomaly, Eu negative

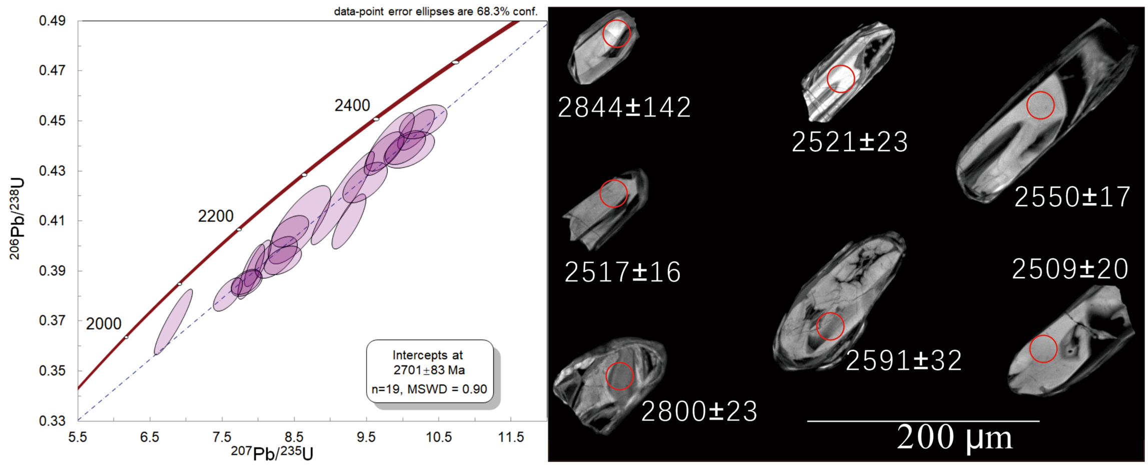

Fig. 2 U–Pb ages of the zircon for the Qinggangping mafic dike (sample HM01)

anomaly, heavy rare earth enrichment, and rare earth loss (Fig. S2) were revealed (Belousova et al. 2002; Xu et al. 2020). The structure and Th/U ratio of the zircons also indicated the magmatic origin of the samples (Belousova et al. 2002; Hoskin and Schaltegger 2018). The LA-ICP-MS zircon analysis results are presented in Table S1 and Fig. 2. A total of 53 zircons were tested, with the oldest being 2843 ± 142 and 2800 ± 23 Ma. Due to the high content of U and Th and the influence of metamorphism, the radioactive lead of magmatic zircon is generally lost, and the data points deviate from the Concordia line and get distributed along the discordia line. After excluding data points with high discordance and that were significantly young, a Concordia diagram for 19 magmatic zircons was obtained, indicating a concordia age of 2701 ± 83 Ma (Fig. 2). The mean squared weighted deviation (MSWD) was calculated to be 0.9.

The present study conducted in-situ Hf isotope analysis of zircons from metamorphic mafic dike samples. The analysis points were situated at the same position as the zircons that had undergone U–Pb age testing conducted at Beijing CreaTech Testing Technology Co., Ltd. (See Supplementary Text for measurement method details). The ^{176}Lu/^{177}Hf ratio ranged from 0.000524 to 0.001025, ^{176}Hf/^{177}Hf ratio ranged from 0.281288 to 0.281411, and ε_{Hf} (t) ranged from 3.5 to 6.6, with an average value of 4.7. In the plots of zircon Hf isotope for the Qinggangping mafic dykes (Fig. 3), all data points were situated between the chondrite and depleted mantle evolution line, indicating that the magma source area had the characteristics of a mantle source material composition. The ε_{Hf} (t) value and Hf model age of all zircon analysis points in the sample were calculated using a single zircon's age as the zircon crystallization age. The zircons yielded two-stage Hf model ages between 2642 and 2922 Ma (Fig. 3), some two-stage model ages are either corresponded with their magma ages

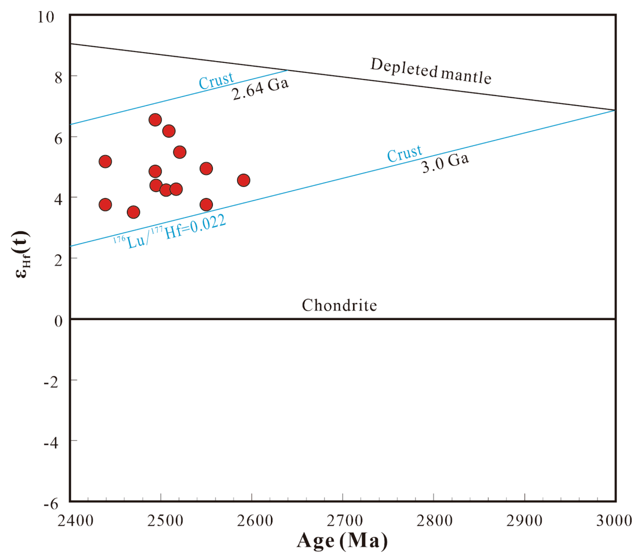

Fig. 3 Plots of zircon Hf isotope corresponding to the Qinggangping mafic dike (sample HM01)

(spots, HM01-06, HM01-20, and HM01-22, Table S3) or slightly earlier than their magma ages (spots: HM01-01, HM01-04, HM01-12, HM01-14, HM01-15, HM01-25, and HM01-30, Table S3), indicating that the basaltic rocks originated directly from the depleted mantle.

The major and trace element analysis of the whole rock samples was conducted at the Aussite Mineral Laboratory using inductively coupled plasma atomic emission spectrometry (ICP-AES) and X-ray fluorescence spectrometry (XRF) techniques. The SiO_2 content of all six samples ranged from 51.48–51.65 wt%, indicating that they belonged to the basalt (Fig. 4a) series magma (Winchester and Floyd 1977). Previous studies have demonstrated that if crustal materials contaminate the mafic magma, the La/Sm ratio would be greater than 5 (Shinjo and Kato 2000), and the Th/La ratio would be greater than 1 (Taylor and

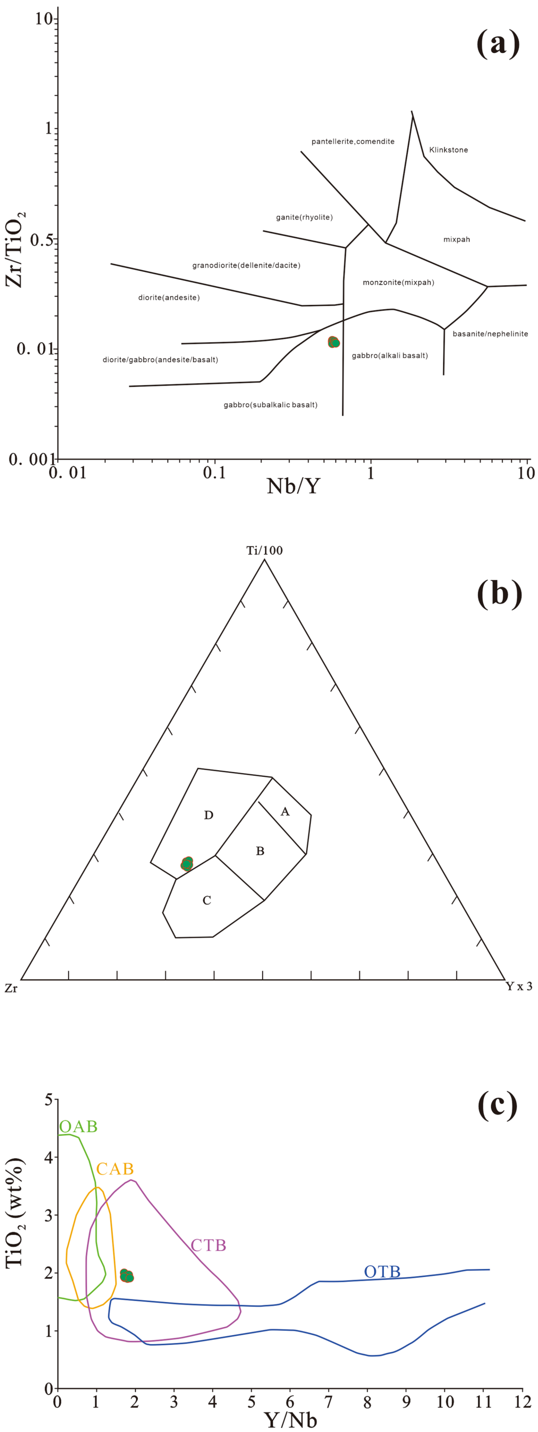

Fig. 4 Tectonic discrimination diagrams for the Qinggangping mafic dike (sample HM01). (**a**) Nb/Y-Zr/TiO_2 diagram (Winchester and Floyd 1977), with the mafic rocks as circles; (**b**) Discrimination diagram based on Ti, Zr, and Y. "Within-plate" basalts (WPB) plot in field D, ocean-floor basalts (OFB) in field B, low-potassium tholeiites (LKT) in fields A and B, and calc-alkali basalts (CAB) in fields C and B (Pearce and Cann 1973; Pearce and Norry 1979); (**c**) TiO_2-Y/Nb diagram. continental alkaline basalt (CAB), oceanic alkaline basalt (OAB), continental tholeiite basalt (CTB), oceanic tholeiitic basalt (OTB) (Floyd and Winchester 1975).

McLennan 1985). The mafic dikes in this study are characterized by La/Sm ratios ranging from 4.63 to 4.79 and Th/La ratios ranging from 0.13 to 0.14, suggesting that crustal materials do not contaminate them during magma rise. Therefore, the element characteristics of these mafic volcanic rocks can effectively reveal their source characteristics and tectonic settings. The samples exhibit relatively high Ti/Y ratios (ranging from 380.89 to 412.73, with an average of 397.21) and low Hf/Ta ratios (ranging from 6.00 to 7.38, with an average of 6.98), indicating that these rocks are similar to intraplate basalts (Condie 1989). On the Ti–Zr–Y discrimination diagram, all six samples fall in the intraplate basalt region (Fig. 4b). The Zr/Nb (ranging from 13.15 to 13.52) and Y/Nb (ranging from 1.72 to 1.82) ratios of the basaltic magmatic rocks (Table S1) are very similar to those of EMORB, Parana, and Etendeka continental tholeiites (Wilson 1989). The TiO_2–Y/Nb discrimination diagram of basalts also indicates a continental tholeiite series (Fig. 4c, after Floyd and Winchester 1975). The dikes have low TiO_2, Al_2O_3, alkali, and high iron contents. They exhibit tholeiite characteristics and are derived from mantle-derived magma.

The stable lithosphere, absence of orogenic activity, and intrusion of ultramafic–mafic dikes are key indicators of cratonization (Zhai and Santosh 2011). In the NCC, after undergoing extensive continental crust accretion (peaking at 2.82 Ga), the cratonization stage of microcontinental assembly occurred during its evolution in the Archean period. At around 2.7 Ga, the NCC reached its maximum lithospheric thickness of approximately 33–62 km, suggesting the presence of a highly stable lithosphere during this period (Sun 2021; Zhai 2011). The emplacement of ultramafic–mafic and alkaline dikes indicates the evolution stage of post-orogenic or non-orogenic and can therefore be used to determine the timing of cratonization (Geng et al. 2006; Li et al. 2010). Prior studies have identified mafic-mafic dikes dating back approximately 2.5 Ga, indicating that cratonization was completed before this time (Li et al. 2010). This study reports the discovery of ancient mafic magmatic rock in the NCC with an intrusive age of zircon in Huozhou diabase at 2701 ± 83 Ma and the oldest zircon age being more than 2.8 Ga. This finding suggests that cratonization may have occurred earlier than 2.7 Ga. The geochemical data from the Huozhou diabase, which is approximately 2.7 Ga old, indicate that it belongs to the category of intraplate basalt and, more specifically, to continental tholeiite. This finding suggests that the diabase was formed within an extensional environment, with the presence of mafic dikes serving as direct evidence of lithospheric extension. Notably, the intruded mafic dike is situated above the TNCO, precisely at the point where the East and West continental blocks merged during the NCC's cratonic process. These observations lead us to conclude that the NCC was in an extension state following the merging of the East and West continental blocks.

2 Conclusions

Based on the age data, Hf isotope analysis, and major and trace element analysis, it can be concluded that the mafic dike, which is approximately 2.7 Ga old, was formed in an extensional environment following cratonization. This finding suggests that cratonization of the NCC was completed around 2.7 Ga ago, and its modern plate tectonics began in the TNCO at that time. The time of cratonization of the NCC is ~ 200 Ma earlier than previously believed, and it is also earlier than the cratonization of most ancient lands in the world, ranging from 2.65 billion to 2.5 Ga (Li et al. 2010; Zhai 2011). This early cratonization time is noteworthy and deserves continued attention from scholars.

Supplementary Information The online version contains supplementary material available at https://doi.org/10.1007/s11631-023-00638-2.

Acknowledgements This research was jointly supported by the open fund from the Key Laboratory of Deep-Earth Dynamics of Ministry of Natural Resources, Institute of Geology, Chinese Academy of Geological Sciences (Award No. J1901-16); the project of graduate education and teaching reform in Shanxi Province (Number 2021YJJG147); the teaching reform project "Geographic Modeling, Simulation and Visualization" established by Shanxi Normal University (Number 2019JGXM-39); "The Research Start-up Fund of Shanxi Normal University for Dr. Peng Chong in 2016" (Award Number 0505/02070438); "The Research Start-up Fund of Shanxi Normal University for Dr. Liu Haiyan in 2017" (Number 0505/02070458); and "The Research Fund for Outstanding Doctor in 2017" (Number 0503/02010168), established by the Education Department of Shanxi Province for Dr. Liu Haiyan.

Author contributions CP conceived and designed the experiments; HL directed the writing of this article. HL perfected English writing and contributed analysis tools; All authors read and approved the final manuscript.

Funding This research was jointly supported by the open fund from the Key Laboratory of Deep-Earth Dynamics of Ministry of Natural Resources, Institute of Geology, Chinese Academy of Geological Sciences (Number J1901-16); the project of graduate education and teaching reform in Shanxi Province (Number 2021YJJG147); the teaching reform project "Geographic Modeling, Simulation and Visualization" established by Shanxi Normal University (Number 2019JGXM-39); "The Research Start-up Fund of Shanxi Normal University for Dr. Peng Chong in 2016" (Number 0505/02070438); "The Research Start-up Fund of Shanxi Normal University for Dr. Liu Haiyan in 2017" (Number 0505/02070458); and "The Research Fund for Outstanding Doctor in 2017" (Number 0503/02010168), established by the Education Department of Shanxi Province for Dr. Liu Haiyan.

Declarations

Conflict of interest The authors declare that they have no competing interest.

References

Belousova E, Griffin W, O'Reilly SY, Fisher N (2002) Igneous zircon: trace element composition as an indicator of source rock type. Contrib Miner Petrol 143(5):602–622

Buchan KL et al (2001) Rodinia: the evidence from integrated paleomagnetism and U-Pb geochronology. Precambr Res 110(1):9–32

Condie KC (1989) Geochemical changes in basalts and andesites across the Archean-Proterozoic boundary: identification and significance. Lithos 23(1–2):1–18

Ernst R, Srivastava R, Bleeker W, Hamilton M (2010) Precambrian Large Igneous Provinces (LIPs) and their dyke swarms: new insights from high-precision geochronology integrated with paleomagnetism and geochemistry. Precambr Res 183(3):vii–xi

Floyd PA, Winchester JA (1975) Magma type and tectonic setting discrimination using immobile elements. Earth Planet Sci Lett 27(2):211–218

Geng Y, Liu F, Yang C (2006) Magmatic event at the end of the archean in Eastern Hebei province and its geological implication. Acta Geol Sin 80(6):15

Halls HC, Zhang B (1998) Uplift structure of the southern Kapuskasing zone from 2.45 Ga dike swarm displacement. Geology 26(1):67–70

Hoek JD, Seitz HM (1995) Continental mafic dyke swarms as tectonic indicators: an example from the Vestfold Hills. East Antarct Precambrian Res 75(3):121–139

Hoskin P, Schaltegger U (2018) The composition of zircon and igneous and metamorphic petrogenesis. Rev Mineral Geochem 53(1):27–62

Hou G (2012) Mechanism for three types of mafic dyke swarms. Geosci Front 3(2):217–223

Kusky TM, Li JH, Tucker RD (2001) The Archean Dongwanzi ophiolite complex, North China Craton: 2.505-billion-year-old oceanic crust and mantle. Science 292(5519):1142–5

Li T, Zhai M, Peng P, Chen L, Guo J (2010) Ca. 2.5 billion year old coeval ultramafic–mafic and syenitic dykes in Eastern Hebei: implications for cratonization of the North China Craton. Precambrian Res 180(3–4):143–155

Pearce JA, Cann JR (1973) Tectonic setting of basic volcanic rocks determined using trace element analyses. Earth Planet Sci Lett 19(2):290–300

Pearce JA, Norry MJ (1979) Petrogenetic implications of Ti, Zr, Y, and Nb variations in volcanic rocks. Contrib Miner Petrol 69(1):33–47

Peng C, Xue LF, Zhu M, Chai Y, Liu WY (2016) The location and evolution of the tectonic boundary between the Paleoproterozoic Jiao-Liao-Ji Belt and the Longgang Block, northeast China. Precambrian Res 272:18–38

Peng C et al (2020) Location of the tectonic boundary between the Paleoproterozoic Jiao–Liao–Ji Belt and the Archean Longgang Block in the Lianshanguan area, northeastern China. Precambr Res 344:105762

Peng C, Pan B, Xue L, Liu H (2021) Does the Liaoji granite represent basement in the Jiao–Liao–Ji Belt? Precambr Res 365:106387

Peng C et al (2023) Geochronological and geochemical constraints on the granitic gneiss in the Huozhou complex: implications for the tectonic evolution of the Trans-North China Orogen. Acta Geochim 42(1):153–181

Shinjo R, Kato Y (2000) Geochemical constraints on the origin of bimodal magmatism at the Okinawa Trough, an incipient back-arc basin. Lithos 54(3):117–137

Stark JC et al (2018) First evidence of Archean mafic dykes at 2.62 Ga in the Yilgarn Craton, Western Australia: links to cratonisation and the Zimbabwe Craton. Precambr Res 317:1–13

Sun G et al (2021) Thermal state and evolving geodynamic regimes of the Meso- to Neoarchean North China Craton. Nat Commun 12(1):3888

Taylor SR, McLennan SM (1985) The continental crust: its composition and evolution

Wang X, Zhu W, Zheng Y, Ge R (2022) Tectonic switch from a lithospheric rift to an active continental margin in the Paleoproterozoic: evidence from low δ18O granites from the Trans-North China Orogen in the North China Craton. Precambr Res 377:106672

Wilson MB (1989) Igneous petrogenesis a global tectonic approach

Winchester JA, Floyd PA (1977) Geochemical discrimination of different magma series and their differentiation products using immobile elements. Chem Geol 20(1):325–343

Xu W, Liu F (2019) Geochronological and geochemical insights into the tectonic evolution of the Paleoproterozoic Jiao-Liao-Ji Belt, Sino-Korean Craton. Earth Sci Rev 193:162–98

Xu H, Luo JH, Ren ZL, Chen GX, Li YF, You J (2020) Geochronology, geochemistry and tectonic significance of Paleoproterozoic diabase at the southwestern margi. Geochronology, geochemistry and tectonic significance of Paleoproterozoic diabase at the southwestern margin of the Ordos Block. Acta Petrol Sin 36(4):1186–1198

Zhai M, Santosh M (2011) The early Precambrian odyssey of the North China Craton: a synoptic overview. Gondwana Res 20(1):6–25

Zhai M et al (2011) Cratonization and the Ancient North China continent: a summary and review. Sci China 54:1110–20

Zhao G et al (2012) Amalgamation of the North China craton: key issues and discussion. Precambr Res 222–223(12):55–76